JOURNAL OF VIROLOGY, May 1985, p. 401–407
0022-538X/85/050401-07$02.00/0

Vol. 54, No. 2

Varying the Position of a Retrovirus Packaging Sequence Results in the Encapsidation of Both Unspliced and Spliced RNAs

RICHARD MANN AND DAVID BALTIMORE*

Whitehead Institute for Biomedical Research, Cambridge, Massachusetts 02142, and Department of Biology, Massachusetts Institute of Technology, Cambridge, Massachusetts 02139

Received 13 December 1984/Accepted 3 January 1985

By using a retroviral construct derived from Moloney murine leukemia virus and capable of expressing the dominant selectable *neo* gene, we measured the effects of moving or deleting a sequence (Ψ) known to be required in *cis* for the packaging of genomic RNA into virus particles. When Ψ was at its wild-type position (in SVX virus) near the 5′ end of the RNA, the titer of infectious virus production was 5×10^6 G-418-resistant CFU per ml. The titer was decreased approximately fivefold when Ψ was moved, in its proper orientation, to near the 3′ end of the virus (SVX-ΨC) and was decreased approximately 600-fold when Ψ was moved, in its proper orientation, into the U3 region of the long terminal repeat. When Ψ was deleted (SVX-Ψ^-) or inserted in the opposite orientation at either of these two positions, the titer was decreased by 3000-fold relative to SVX. In SVX-ΨC, Ψ was no longer in the intron (as it is in SVX and Moloney murine leukemia virus) but was moved to a region which is only exonic. This resulted in the encapsidation of both spliced and unspliced RNAs, their efficient reverse transcription, and their integration into the genome of an infected cell. A number of proviruses resulting from integration of either spliced or unspliced RNAs were cloned. Four of these clones were subjected to sequence analysis in the region of the splice sites, and it was determined which sites are used by these viruses and also which are used by Moloney murine leukemia virus.

For retroviruses to complete a cycle of infection, a number of *cis*-acting genomic sequences are required. These include enhancer, promoter, and polyadenylation signals which are needed for proper mRNA synthesis and processing (1, 12, 29), primer binding sites required for reverse transcription (7, 16, 18, 24), and signals needed for the efficient and specific encapsidation of genomic RNA molecules into virus particles (14, 19, 25, 26, 30).

We previously have reported the identification of a sequence (Ψ) of Moloney murine leukemia virus (M-MuLV) which, when deleted, reduced the packaging of genomic RNA into virions to below detectability (14). Similar sequences have been identified in two avian viruses, spleen necrosis virus (30) and Rous sarcoma virus (19, 25). In M-MuLV, this sequence is located in a 350-base-pair (bp) fragment just upstream from the initiation codon of $Pr65^{gag}$. The exact size of Ψ is not known, but deletion analysis demonstrates that the 3′-most 210 nucleotides of the 350-bp fragment are not required for it to function (22; R. Mann, unpublished data). M-MuLV genomes lacking Ψ are defective only in *cis* because they can still direct the synthesis of all viral proteins required for the assembly and budding of infectious virus.

To extend our study of the role of Ψ, we used a plasmid encoding a defective derivative of M-MuLV (SVX) which is capable of expressing the bacterial neomycin resistance gene (*neo*) (2). This gene is a dominant selectable marker in mammalian cells because it confers resistance to the compound G-418 (5, 8). SVX also contains pBR322 and simian virus 40 (SV40) sequences which allow for the efficient rescue from cells of its proviral form.

Deletion of Ψ from pSVX, the plasmid encoding SVX virus, greatly reduced the titer of the virus, and replacement of Ψ in two new positions resulted in intermediate titers. Movement of Ψ away from its normal site in the intron of SVX to a site that is not removed during splicing resulted in the packaging of spliced RNA molecules. This has allowed a detailed analysis of the splice sites used by SVX and M-MuLV to generate subgenomic mRNAs.

MATERIALS AND METHODS

Cells and viruses. NIH/3T3 fibroblasts, Ψ2 cells (14), and all lines derived by viral infection were grown in Dulbecco-modified Eagle medium supplemented with 10% calf serum at 37°C in an atmosphere of 5% CO_2. Viral infections were carried out in the presence of 8 μg of polybrene per ml at 37°C for 2 h. Selection for G-418-resistant clones was done by splitting the population of infected or transfected cells at a ratio of 1:20 into the medium described above plus 1 mg of G-418 (GIBCO Laboratories) per ml. Individual clones were isolated by the use of cloning cylinders and were grown in the presence of 1 mg of G-418 per ml for at least 5 more days. A population of G-418-resistant clones was obtained by growth in mass culture of all clones which grew in one or more of the selection dishes.

Cloned DNAs. Plasmid pSVX has been described by Cepko et al. (2). pSVX-Ψ^- was constructed by using *Bam*HI linkers to change the *Hin*dIII site (at 0.7 units) of pMOV-Ψ^- (14) to a *Bam*HI site. A long terminal repeat (LTR)-containing the *Xba*I to *Bam*HI fragment was isolated by preparative low melt agarose gel electrophoresis and inserted into pSVX in place of the approximately 0.7-kilobase-pair (kb) *Xba*I to *Bam*HI fragment, thus incorporating the Ψ^- deletion into the SVX virus. pSVX-ΨC (proper orientation of Ψ) and pSVX-$\overline{\Psi}$C (opposite orientation of Ψ) were constructed by ligating a blunted, *Cla*I-linkered *Bal*I (0.7 units) to *Pst*I (1.0 units) fragment of pMOV-9 (4) into the unique *Cla*I site of pSVX-Ψ^-. pSVX-ΨX (proper orientation of Ψ) and pSVX-$\overline{\Psi}$X (opposite orientation of Ψ) were constructed by ligating this same fragment, linked with *Xba*I, into the *Xba*I site in the 3′ LTR of pSVX-Ψ^-. All linkers were obtained from Collaborative Research, Inc.

* Corresponding author.

Derivation of cell lines. The cell line SVX/Ψ2-9, which produces SVX virus, was generated by transfecting Ψ2 cells with pSVX, selecting for G-418 resistance, and picking independent colonies. SVX/Ψ2-9 produced the highest titer among 15 such clones. The cell line ΨC/Ψ2-9, which produces SVX-ΨC virus, was generated by transfecting Ψ2 cells with pSVX-ΨC, selecting for G-418 resistance and picking independent colonies. ΨC/Ψ2-9 produced the highest titer among 15 such clones. Ψ^-/Ψ2-1 and Ψ^-/Ψ2-2, which produce SVX-Ψ^- virus, were generated by transfecting Ψ2 cells with pSVX-Ψ^-, selecting for G-418 resistance and picking independent colonies. The cell lines SVX-1 and SVX-2 were derived by infecting NIH/3T3 cells with supernatants from Ψ2 cells that had been transfected with pSVX 20 h earlier (transiently derived virus). The cell lines ΨC-1, ΨC-2, and ΨC-3 were derived by infecting NIH/3T3 cells with supernatants from Ψ2 cells that had been transfected with pSVX-ΨC 20 h earlier (transiently derived virus). The cell lines ΨC9-3 and ΨC9-6 were derived by infecting NIH/3T3 cells with virus obtained from the ΨC/Ψ2-9 cell line. In all of the infections described above, the NIH/3T3 cells were selected for G-418 resistance, and independent colonies were picked.

Analysis of cellular DNA. High-molecular-weight DNA was isolated from tissue culture cells as described previously (13), and portions were digested with the appropriate restriction endonucleases and ethanol precipitated. The DNA fragments were separated in a horizontal agarose gel in Tris-borate buffer as described previously (13) and transferred to nitrocellulose filters (Schleicher & Schuell, Inc.) as described previously (13). The immobilized DNA was hybridized to pSV2neo (27) plasmid that was ^{32}P-labeled by nick-translation (13). The hybridization and wash conditions were as described previously (13).

Mammalian cell transfections and transformations. The method of mammalian cell transfection and transformation employed here was identical to that used by Mann et al. (14).

Preparation of RNA. Total cellular RNA was prepared as described previously (3). Virion RNA was prepared by phenol extraction of virions banded in a sucrose step gradient (24).

S1 nuclease analysis. Twenty micrograms of total RNA was hybridized in 20 μl of hybridization buffer (10) with a DNA fragment labeled at the 5′ end with ^{32}P. The hybridization was at 48°C for 12 to 16 h. The hybrids were digested with 50 units of S1 nuclease (P-L Biochemicals, Inc.) at 37°C for 1 h in 400 μl of S1 buffer. The protected DNA fragments were separated by electrophoresis through 6% polyacrylamide-urea gels which were exposed to X-ray film (Kodak XAR5) with an intensifying screen (Du Pont Lightning Plus) at −70°C. The fragment labeled at the 5′ end with ^{32}P was prepared by digestion of pSVX with *Xho*I followed by removal of the 5′-terminal phosphate with calf intestinal phosphatase (Boehringer Mannheim Corp.). The DNA was labeled with T4 polynucleotide kinase (Bethesda Research Laboratories) and [γ-^{32}P]ATP (ICN Pharmaceuticals, Inc.) and was then digested with *Xba*I. The Ψ-containing, end-labeled fragment was isolated by electrophoresis on a 1% low melt agarose gel.

Cloning of integrated proviruses. The method for cloning SVX proviruses was as described by Cepko et al. (2). Briefly, the cell line harboring the provirus to be cloned was co-plated with SV40 T-antigen containing COS cells. The plate was grown to confluence, and the cells were fused with polyethylene glycol. After 2 days of incubation, low-molecular-weight DNA was isolated by the removal of the Hirt precipitate with a centrifuge. The supernatant was phenol extracted and ethanol precipitated. A portion of the redissolved material was used to transfect *Escherichia coli* HB101 followed by selection for kanamycin resistance. In general, plasmid from six kanamycin-resistant colonies was isolated for each proviral cloning to ensure that the plasmid structure accurately represented the proviral structure.

DNA sequence analysis. Plasmids whose splice site regions were to be sequenced were digested with *Ava*II and the fragment containing the splice sites was isolated by preparative low melt agarose gel electrophoresis. The *Ava*II fragments were end labeled as described above for the preparation of the S1 nuclease probe. The labeled fragments were strand separated as described previously (13), and both strands were subjected to sequencing reactions by the method of Maxam and Gilbert (15). The products were electrophoresed through 8% polyacrylamide urea gels, which were then exposed to X-ray film with an intensifying screen at −70°C.

RESULTS

To determine whether the sequence required in *cis* for encapsidation of genomic RNA into virus particles (Ψ) can function at more than one location, we varied its position along the RNA and studied these variants in a series of transfection experiments. The proviral structures of these variants are illustrated in Fig. 1. The parent plasmid pSVX had its packaging site in the wild-type position (2). This position is between the 5′ and 3′ splice sites of this virus and, therefore, will be considered part of an intron. This intron is unusual because it is removed from only about one-half of the transcripts (see below). pSVX and its derivatives are capable of expressing the dominant selectable marker (*neo*) which confers resistance to kanamycin in bacteria and to the drug G-418 in mammalian cells (5, 8). The first variant, pSVX-Ψ^-, had a deletion of the 350-bp fragment previously identified to contain a *cis* packaging sequence (14). pSVX-ΨC had the same deletion as pSVX-Ψ^- but also had the 350-bp fragment translocated in its proper orientation to the *Cla*I site near the 3′ end of the provirus. pSVX-ΨX had the 350-bp fragment translocated to the *Xba*I site in the 3′ LTR. Each of these plasmids was transfected into the Ψ2 packaging cell line (14), and virus production was measured by two assays. The transient assay consisted of determination of the titer of G-418-resistant CFU per milliliter (G-418^r CFU/ml) by infection of NIH/3T3 cells with culture supernatants obtained 20 h posttransfection. The stable assay involved

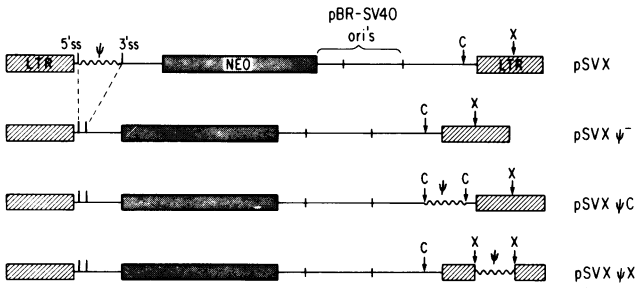

FIG. 1. Structure of the proviral forms of SVX and its derivatives. SVX has Ψ in the wild-type position, SVX-Ψ^- has Ψ deleted, SVX-ΨC has Ψ inserted in the proper orientation at the *Cla*I site, and SVX-ΨX has Ψ inserted in the proper orientation at the *Xba*I site. Abbreviations: C, *Cla*I; X, *Xba*I; ss, splice site; the LTRs, *neo* gene, and pBR322 (pBR) plus SV40 origins of replication are indicated.

determination of the titer of G-418^r CFU/ml by infection of NIH/3T3 cells with culture supernatants from a population of stable G-418^r Ψ2 transfectants. Each population consisted of 100 to 200 independent G-418^r events to minimize differences due to the position or copy number of the transfected DNA. All plasmids were capable of generating G-418^r virus to grossly varying degrees (Table 1). With pSVX as the standard, pSVX-ΨC was approximately four- to sixfold less efficient, pSVX-ΨX was about 600-fold less efficient, and pSVX-Ψ$^-$ was about 3000-fold less efficient at producing G-418^r CFU when transfected into Ψ2 cells. Plasmids in which the packaging site was inserted in the opposite orientation at the *Cla*I (pSVX-$\overline{\Psi}$C) or the *Xba*I (pSVX-$\overline{\Psi}$X) sites yielded titers equivalent to those of pSVX-Ψ$^-$.

The proviral structure of G-418-resistant NIH/3T3 clones infected with transiently obtained SVX or SVX-ΨC virus was analyzed by restriction enzyme cleavage and hybridization with ^{32}P-labeled *neo* sequences (Fig. 2). Two independently obtained SVX-infected cell lines (SVX-1 and SVX-2) yielded the expected fragments on digestion with *Bam*HI plus *Xba*I (3.5-kb; lanes 1 and 2, Fig. 2) and with *Eco*RI plus *Xba*I (2.8-kb; lanes 6 and 7, Fig. 2). Two patterns were obtained among three independent SVX-ΨC-infected cell lines. ΨC-1 had the expected structure, generating a 3.8-kb band on *Bam*HI plus *Xba*I digestion (lane 3, Fig. 2) and a 2.5-kb band on *Eco*RI plus *Xba*I digestion (lane 8, Fig. 2). ΨC-2 and ΨC-3 had different structures: a 4.0-kb band on *Bam*HI plus *Xba*I digestion (lanes 4 and 5, Fig. 2) and a 2.4-kb band on *Eco*RI plus *Xba*I digestion (lanes 9 and 10, Fig. 2). This novel pattern could be explained by a small deletion within the provirus which removed the *Bam*HI site. Thus, the *Bam*HI plus *Xba*I digest would result in a 4.0-kb *Xba*I to *Xba*I hybridizable fragment, and the *Eco*RI plus *Xba*I digest would yield a 2.4-kb fragment because of a deletion of approximately 100 bp.

A splice between M-MuLV 5′ and 3′ splice sites in SVX-ΨC could account for the small deletion that removed the *Bam*HI site and resulted in the proviral structure found in the ΨC-2 and ΨC-3 cell lines (Fig. 2). Such an interpretation implies that spliced SVX-ΨC RNA can be packaged into virus particles, can be efficiently reverse transcribed, and can be integrated into the genome of an infected cell. To directly test whether spliced RNAs were encapsidated in a stable SVX-ΨC producer cell line (ΨC/Ψ2-9), an S1 nuclease analysis was used (Fig. 3). Cellular RNA from a cell line producing standard SVX virus (SVX/Ψ2-9) protected a 950-bp fragment corresponding to unspliced RNA (band I, Fig. 3) and a 280-bp fragment corresponding to spliced RNA (band III, lane 1, Fig. 3). The intensities of these two bands ranged, among a number of experiments, from a ratio of 1:1 to 1:5 of unspliced:spliced RNA. This demonstrates that, as in M-MuLV, a significant amount of retroviral RNA, at steady state, remains unspliced. SVX virion RNA protected only a 950-bp fragment of probe DNA (lane 2, Fig. 3). Other faint bands seen in these two lanes were probably due to protection by specific degradation products of the unspliced RNA.

TABLE 1. Production of virus (G-418^r CFU) by pSVX and its derivatives

Plasmid	Titer of virus produced (CFU/ml)	
	Transient	Stable
pSVX	850	4.0×10^6
pSVX-Ψ$^-$	<10[a]	1.2×10^3
pSVX-ΨC	150	1.0×10^6
pSVX-ΨX	<10[a]	7.0×10^3
pSVX-$\overline{\Psi}$C	<10[a]	1.2×10^3
pSVX-$\overline{\Psi}$X	<10[a]	1.1×10^3

[a] No G-148^r CFU were observed.

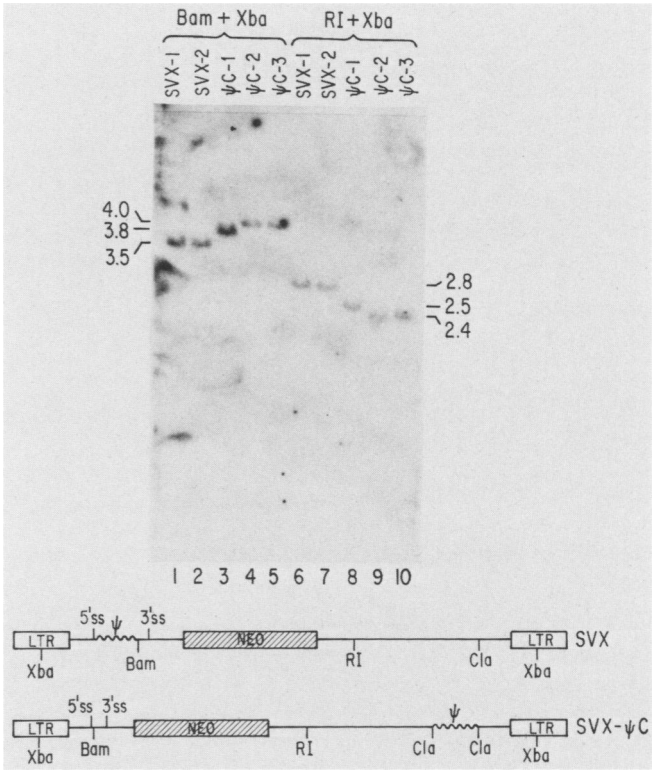

FIG. 2. Hybridization analysis of G-418^r cell lines infected with SVX or SVX-ΨC virus. SVX-1 and SVX-2 were derived by infection of NIH/3T3 cells with transiently obtained SVX virus. Ψ-1, Ψ-2, and Ψ-3 were derived by infection of NIH/3T3 cells with transiently obtained SVX-ΨC virus. Abbreviations: Bam, *Bam*HI; RI, *Eco*RI; Xba, *Xba*I; Cla, *Cla*I; ss, splice site. The structures of SVX and SVX-ΨC are shown with the relevant restriction endonuclease sites. Numbers to the right and left of the gel are in kb.

Cellular RNA from a cell line producing SVX-ΨC virions (ΨC/Ψ2-9) protected a 380-bp fragment corresponding to unspliced RNA (band II, Fig. 3) and a group of three bands (band III, Fig. 3), ranging from about 295 to 270 bp, which, as will be shown below, correspond to different spliced RNA species (lane 3, Fig. 3). SVX-ΨC virion RNA protected both unspliced (band II, Fig. 3) and spliced (band III, Fig. 3) RNAs (lane 4, Fig. 3). Therefore translocation of the 350-bp Ψ fragment from the intron of the virus to the exon sequences at *Cla*I resulted in the encapsidation of both spliced and unspliced RNAs in contrast to virus with Ψ in intron sequence which packaged only unspliced RNA.

The proviral form of the SVX virus family can be easily cloned in *E. coli* (see Cepko et al. [2] for a detailed description). This was done for a number of G-418^r NIH 3T3-infected cell lines harboring SVX, SVX-Ψ$^-$ or SVX-ΨC proviruses (Table 2). By restriction endonuclease analysis four of four cloned SVX proviruses had a structure identical to that of the original SVX construction; i.e., no rearrangements were observed. Cloned SVX-ΨC proviruses were of two general structures: either identical to the original SVX-ΨC construction (three of nine) or equivalent to a cDNA copy of spliced SVX-ΨC RNA (six of nine). The structure of

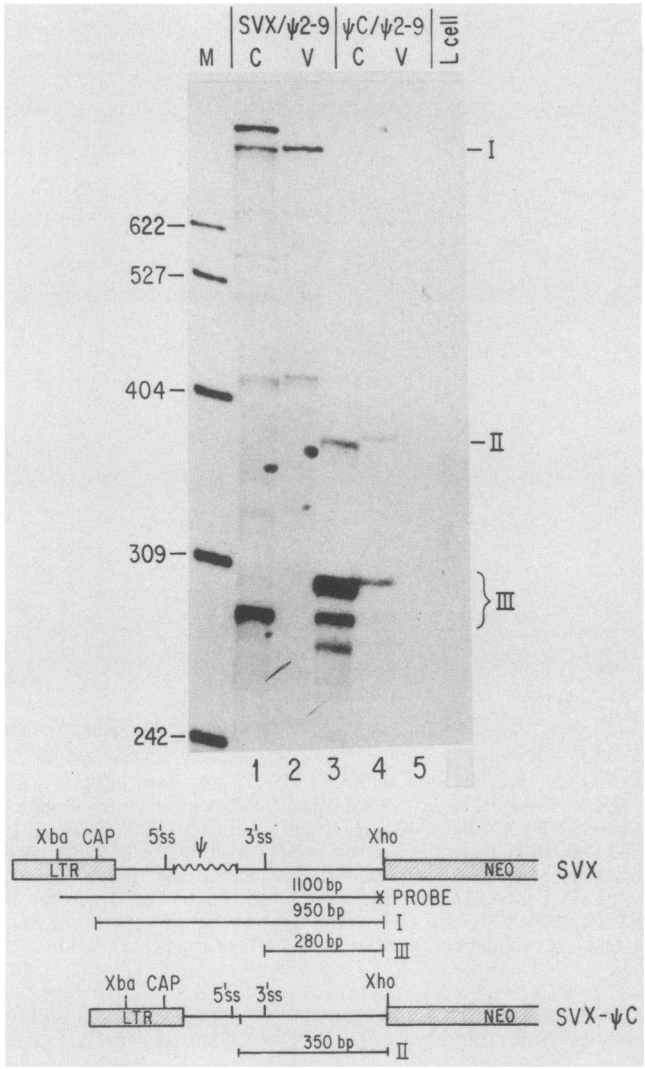

FIG. 3. S1 nuclease analysis of cellular and viral RNAs from a SVX producer line (SVX/Ψ2-9) and a SVX-ΨC producer line (ΨC/Ψ2-9). Abbreviations: M, marker; C, cellular RNA; V, virion RNA; ss, splice site. L cell RNA (lane 5) was used as a negative control. Band I corresponds to full-length SVX RNA, band II corresponds to full-length SVX-ΨC RNA, and band III corresponds to spliced RNA from both SVX and SVX-ΨC. The structure of the relevant regions of the two viruses are shown with the S1 nuclease probe and expected sizes of the various protected fragments. CAP is the site of initiation for RNA synthesis. Numbers to the left of the gel are the sizes of the marker bands in bases.

cloned SVX-Ψ⁻ proviruses were also either identical to the input plasmid (four of seven) or equivalent to a cDNA of spliced SVX-Ψ⁻ RNA (three of seven) (Table 2). In all seven cases examined, proviruses derived from SVX-Ψ⁻ virus did not contain a Ψ sequence, as determined by restriction mapping of the cloned proviruses.

Four of the cloned SVX-ΨC proviruses were sequenced in the region around the splice sites (Fig. 4). Two unspliced proviruses (one from ΨC-1, infected with transiently derived virus, and one from ΨC9-3, infected with ΨC/Ψ2-9 virus) had identical sequences in the *Ava*II fragment containing the splice sites. Sequences of two spliced SVX-ΨC proviruses differed by 14 nucleotides because of the use of two different 3′ splice sites (Fig. 4). The provirus in ΨC9-6, which was derived by infection with ΨC/Ψ2-9 virus, used a 3′ splice site designated B, whereas the provirus in ΨC-2, which was derived by infection with transiently obtained virus, used a 3′ splice site designated A. The choice of 3′ splice site A, but not B, created a *Sac*I restriction endonuclease recognition sequence (Fig. 4). Thus, all other cloned proviruses that were derived from spliced RNA could be screened to determine which 3′ splice site was used by screening for the presence of the *Sac*I site. The presence of the *Sac*I site was taken as strong evidence that 3′ splice site A had been used. Only proviruses generated by virus obtained from the ΨC/Ψ2-9 cell line lacked the *Sac*I recognition sequence at the splice joint, suggesting that the use of 3′ splice site B is peculiar to that cell line (Table 2).

The S1 nuclease pattern of the ΨC/Ψ2-9 cell line was peculiar in that three protected fragments were generated which all mapped close to the 3′ splice site (band III, Fig. 3). Because spliced proviruses generated from ΨC/Ψ2-9 virus used 3′ splice site B, it seemed likely that the largest and most abundant band in this triplet would correspond to this splice site. Similarly, the next smaller band, which appears identical in size to the band present in lane 1 (Fig. 3) (the 3′ splice site used in SVX), would correspond to 3′ splice site A. This was demonstrated by S1 nuclease analysis of cellular RNAs from the various G-418ʳ-infected cell lines harboring those SVX-ΨC proviruses which had been cloned and sequenced (Fig. 5). Lanes 1 and 2 in Fig. 5 repeat the S1 protection patterns of the SVX/Ψ2-9 and ΨC/Ψ2-9 producer cell lines that were seen previously (Fig. 3, lanes 1 and 3). Cell line ΨC9-6, which by sequence analysis had a provirus generated from an RNA spliced to 3′ splice site B, generated the largest of the triplet of protected bands on S1 analysis (lane 4, Fig. 5). Cell line ΨC-2, which by sequence analysis had a provirus generated from a spliced RNA that used 3′ splice site A, generated the middle band of the triplet on S1 analysis (lane 6, Fig. 5). This band is identical to that protected by RNA from SVX/Ψ2-9 (lane 1, Fig. 5). The 3′ splice site A was also used in cell lines ΨC-1 (lane 3, Fig. 5) and ΨC9-3 (lane 5, Fig. 5). These cell lines also contained full-length SVX-ΨC RNA (i.e., protected the 380-bp fragment) because they harbored an unspliced provirus. Among all the cell lines infected with ΨC/Ψ2-9 virus, none harbored a provirus which corresponded to an RNA capable of protecting the smallest of the fragments present in lane 2 (Fig. 5). This is probably due to the low abundance of this RNA relative to the other SVX-ΨC RNAs in the ΨC/Ψ2-9 cell line.

TABLE 2. Cloned proviruses

DNA	Source of virus	Titer (CFU/ml)[a]	No. of proviruses with the following structure	
			Unspliced	Spliced (A or B)[b]
pSVX	Transient	1×10^3	1	0
	SVX/Ψ2-9	5×10^6	3	0
pSVX-Ψ⁻	Transient	$<10^c$	0	0
	Ψ⁻/Ψ2-1	1×10^3	2	1 (A)
	Ψ⁻/Ψ2-1	4×10^2	2	2 (A)
pSVX-ΨC	Transient	2×10^2	1	2 (A)
	ΨC/Ψ2-9	1×10^6	2	4 (B)

[a] Titer is G-418ʳ CFU/ml of culture supernatant.
[b] A or B refers to which 3′ splice site was used.
[c] No G-418ʳ CFU were observed.

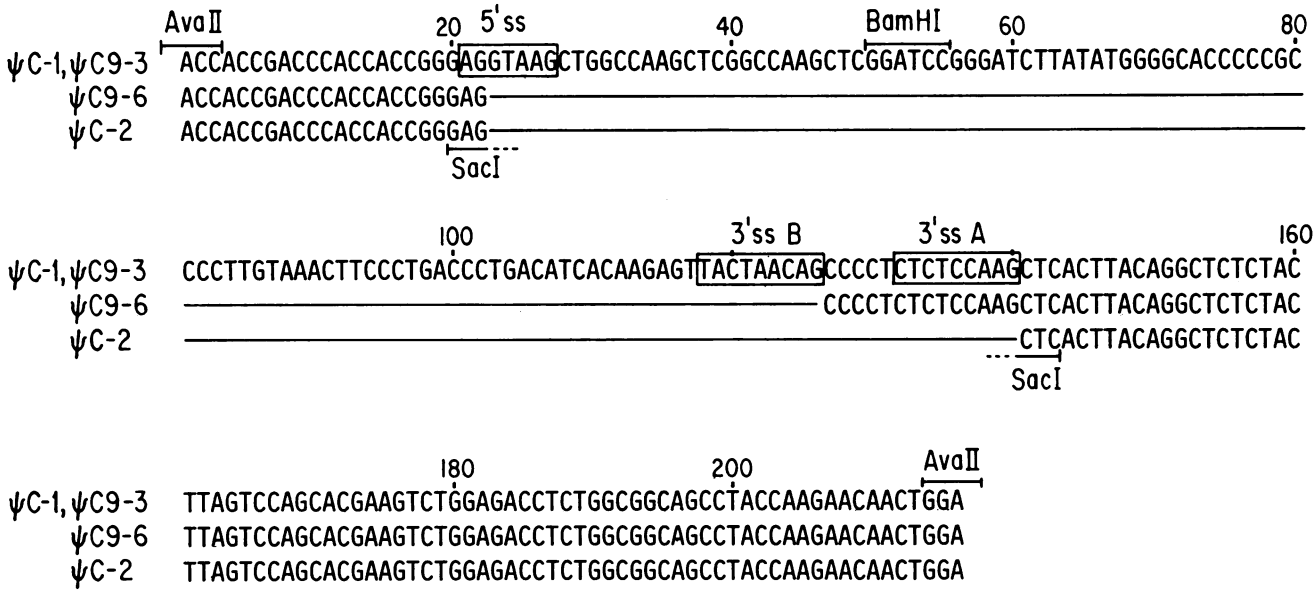

FIG. 4. Sequence comparison of the splice site region from four SVX-ΨC proviruses. Consensus sequences (as compiled in references 23 and 17) for the 5′ splice site and two 3′ splice sites (A and B; see text) are boxed. A solid line represents the absence of nucleotides. ΨC-1 (unspliced) and ΨC-2 (spliced) are derived from transiently derived virus. ΨC9-3 (unspliced) and ΨC9-6 (spliced) are derived from virus obtained from the producer line ΨC/Ψ2-9. The *Ava*II (where sequencing began), *Sac*I (present only in ΨC-2), and *Bam*HI restriction endonuclease sites are shown.

DISCUSSION

Having previously shown that a 350-bp fragment (Ψ) of M-MuLV is required in *cis* for encapsidation of genomic RNA into virions (14), we show here that this fragment can function in a variety of positions within the viral genome. When Ψ is at the *Cla*I site in pSVX-ΨC, the virus titer was only fivefold lower than when Ψ was in its wild-type position. SVX-ΨX virus had a much lower titer than wild-type SVX virus but clearly above that of SVX-Ψ$^-$, the virus from which the entire 350-bp fragment had been deleted. The relatively poor transmission efficiency of SVX-ΨX virus may or may not be due to an encapsidation problem because deleterious effects on other steps in the retroviral life cycle would also adversely affect the G-418^r CFU titer. One potential problem in SVX-ΨX is that the inserted Ψ sequence separates the viral enhancer (12) from the promoter elements which may result in a reduction in the transcription of the *neo* gene.

The ability to translocate Ψ from near the 5′ end of viral RNA to near the 3′ end demonstrates that the Ψ function is relatively autonomous of neighboring sequences. The function of Ψ is not, however, completely independent of position. A fivefold lower titer was produced when Ψ was at the *Cla*I site, which may either be a consequence of partial occlusion by the surrounding sequence or an indication that Ψ acts more efficiently when it can interact with the correct neighboring sequences.

Although producer cell lines harboring the pSVX-Ψ$^-$ plasmid yield G-418^r CFU 3000-fold less efficiently than cell lines containing wild-type pSVX, it was surprising that the SVX-Ψ$^-$ titers were as high as 10^3 CFU/ml (Table 1). This titer is a measure of the leakiness of the 350-bp Ψ$^-$ deletion mutation because these genomes are packaged without a Ψ sequence. This number may also reflect the leakiness of packaging mutations incorporated into replication competent retroviruses (6, 14, 26) and should be considered when these systems are to be used to generate "helper-free" retroviral stocks. If Ψ$^-$ helper genomes are packaged with a similar efficiency to SVX-Ψ$^-$ RNA, then these RNAs could be substrates for recombination with Ψ$^+$ RNAs to generate fully competent helper virus. The Ψ2 cell line, which is such a system for producing helper-free stocks, has not been observed to yield wild-type M-MuLV even with high titer infections (R. Mann and R. Mulligan; unpublished data). This apparent inconsistency suggests that the M-MuLV genome present in Ψ2 may harbor a mutation in addition to the 350-bp Ψ deletion which reduces the propensity of the helper genome to generate wild-type virus to below detectability. The second mutation need not affect packaging; it could also prevent reverse transcription or integration. (In our previous study [14] we reported that transfection of pMOV-Ψ$^-$ [an M-MuLV proviral clone with Ψ deleted] into NIH/3T3 cells eventually resulted in the production of wild-type virus, although at a much slower rate than transfection of the wild-type clone pMOV-Ψ$^+$. With other preparations of pMOV-Ψ$^-$ plasmid, however, production of wild-type virus has not been observed, suggesting that the original plasmid preparation may have had a small amount of contaminating pMOV-Ψ$^+$ plasmid.)

The 10^3 G-418^r CFU SVX-Ψ$^-$ titer may imply that there are other signals on retroviral genomic RNA that are important for packaging. The avian retrovirus, Rous sarcoma virus, appears to have at least two sites that are each necessary for encapsidation. One site is located within the *gag* coding sequence, about 140 nucleotides downstream from the 5′ splice site (19). A second site resides within a 115-nucleotide sequence which is present both upstream and downstream of the v-*src* gene (25). These sites may act coordinately in providing genomic RNA with the proper specificity required for efficient packaging.

By moving the 350-bp Ψ fragment from the intron of pSVX to a site where it is not removed by splicing (in pSVX-ΨC), spliced and unspliced RNAs could be efficiently

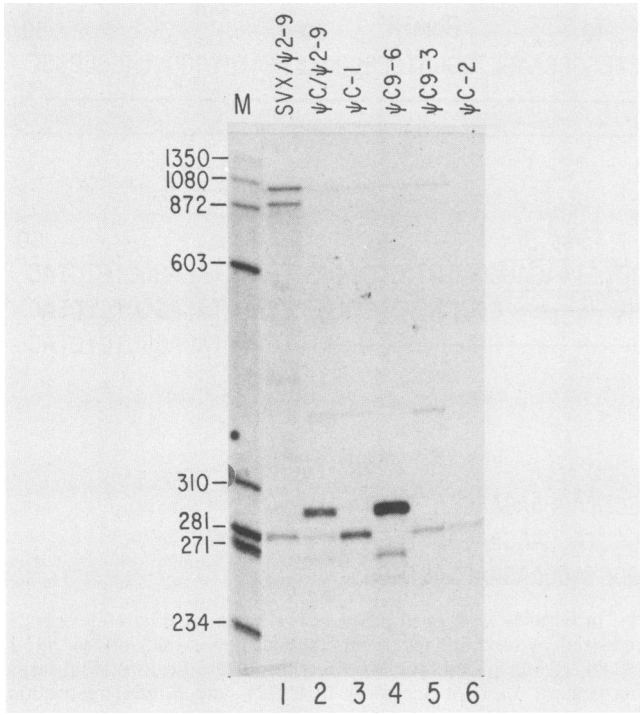

FIG. 5. S1 nuclease analysis of cellular RNAs from producer and infected cell lines. Lanes 1 and 2, RNAs from SVX/Ψ2-9 (producer of SVX virus) and ΨC/Ψ2-9 (producer of SVX-ΨC virus), respectively; lanes 3 and 6, RNAs from ΨC-1 and ΨC-2, respectively (generated by infection with transiently derived SVX-ΨC virus); lanes 4 and 5, RNAs from ΨC9-6 and ΨC9-3, respectively (generated by infection with SVX-ΨC virus from the ΨC/Ψ2-9 producer cell line). The S1 probe is identical to that used in Fig. 3. M, Marker. Numbers to the left of the gel are the sizes of the marker bands in bases.

encapsidated, reverse transcribed, and integrated into the genome of an infected cell. We have used this fact, coupled with the ease of cloning proviruses of SVX and its derivatives, to analyze in detail the splice sites which these viruses use. The splice sites present in pSVX are identical to those in M-MuLV, except for an approximately 5-kb deletion of intronic sequence (from *Pst*I [1.0 unit] to *Bgl*II [5.9 units]), leaving an intron of about 460 nucleotides. The intron present in pSVX-Ψ⁻ and pSVX-ΨC is further reduced to about 110 nucleotides because of the deletion of the Ψ fragment. The splicing reaction for all three of these constructs yields approximately 30% unspliced and 70% spliced RNA (Fig. 2, Table 2) as does the splicing reaction in the wild-type situation of M-MuLV (9, 21). Therefore, deletion of 98% of the intron does not measurably affect the efficiency of splicing. These results support previous studies on the β-globin gene which indicate that no specific internal intron sequence is required for accurate splicing (20, 31). In contrast, however, Hwang et al. (11) have reported recently the existence of two regions of the M-MuLV intron which, when either is deleted, adversely affect splicing. These regions are absent from all of the SVX viruses studied here without affecting splicing. The inefficient splicing described by Hwang et al., therefore, is likely due to some peculiarity of their constructions, such as the particular secondary structure of the RNAs transcribed from them, and probably is not due to the absence of a sequence essential for splicing.

Two 3′ splice sites, separated by only 14 nucleotides, were observed in these studies. The more predominant one (3′ splice site A) is used by SVX (lane 1, Fig. 5), SVX-Ψ⁻ and SVX-ΨC (Table 2) and therefore is probably the site used by M-MuLV. The only situation in which 3′ splice site B was used was in the producer line ΨC/Ψ2-9 or in lines derived from ΨC/Ψ2-9 virus (Fig. 5, Table 2). This suggests that at least one of the copies of the pSVX-ΨC construct introduced by transfection into this line harbored a mutation which activated this normally cryptic splice site. Activation of cryptic splice sites has been observed in a variety of genes and can result from mutations at the normal splice site or at the newly activated splice site (28, 32). The ΨC/Ψ2-9 cell line must also contain at least one copy of an unmutated SVX-ΨC genome because the cell line ΨC9-3, which was infected by ΨC/Ψ2-9 virus, contained an unspliced provirus which used only 3′ splice site A (Fig. 5). The ΨC/Ψ2-9 cell line, therefore, probably expresses two types of SVX-ΨC genomes: one which produces large amounts of RNA spliced to 3′ splice site B (as in lane 4, Fig. 5) and one which splices to 3′ splice site A (as in lane 5, Fig. 5).

The smallest fragment protected by ΨC/Ψ2-9 RNA (lane 2, Fig. 5), may correspond to another spliced RNA that has chosen a second cryptic 3′ splice site. Because no provirus corresponding to this RNA was observed, it cannot be determined whether this RNA is, in fact, a third spliced species. It is peculiar that this same fragment is protected by ΨC9-6 RNA (lane 4, Fig. 5). In this cell line, the provirus is derived from an RNA spliced to 3′ splice site B. Therefore, the usual 5′ splice site should no longer be available to generate any other spliced RNAs.

Although the packaging sequence is able to function at sites other than its wild-type position, there may be other reasons which make some positions more favorable than others. When Ψ is at *Cla*I (in SVX-ΨC), RNA is efficiently packaged, but no distinction is made between the packaging of unspliced and spliced RNAs because both species contain the 350-bp Ψ fragment. In M-MuLV, with Ψ at its wild-type position, the packaging signal is removed during the production of the spliced *env* mRNA, preventing the *env* gene from being transmitted by itself to an infected cell. Transmission of an *env*-only retroviral RNA would be detrimental to the spread of M-MuLV because expression of the *env* protein alone could block any further infection by M-MuLV.

ACKNOWLEDGMENTS

This work was supported by Public Health Service grant CA26717 from the National Cancer Institute.

LITERATURE CITED

1. **Benz, E., Jr., R. Wydro, B. Nadal-Ginard, and D. Dina.** 1980. Moloney murine sarcoma proviral DNA is a transcriptional unit. Nature (London) **288**:665–669.
2. **Cepko, C., B. Roberts, and R. Mulligan.** 1984. Construction and applications of a highly transmissible murine retrovirus shuttle vector. Cell **37**:1053–1062.
3. **Chirgwin, J., A. Przbyla, R. MacDonald, and W. Rutter.** 1979. Isolation of biologically active ribonucleic acid from sources enriched in ribonuclease. Biochemistry **18**:5294–5299.
4. **Chumakov, I., H. Stuhlmann, K. Harbers, and R. Jaenisch.** 1982. Cloning of two genetically transmitted Moloney leukemia proviral genomes: correlation between biological activity of cloned DNA and viral genome activation in the animal. J. Virol. **42**:1088–1098.
5. **Colbere-Garapin, F., F. Hordniceanu, P. Kourilsky, and A. Garapin.** 1981. A new dominant hybrid selective marker for higher eukaryotic cells. J. Mol. Biol. **150**:1–14.
6. **Cone, R., and R. Mulligan.** 1984. High-efficiency gene transfer into mammalian cells: generation of helper-free recombinant

retrovirus with broad mammalian host range. Proc. Natl. Acad. Sci. U.S.A. **81**:6349–6353.
7. **Cordell B., E. Stavnezer, R. Friedrich, J. Bishop, and H. Goodman.** 1976. Nucleotide sequence that binds primer for DNA synthesis to the avian sarcoma virus genome. J. Virol. **19**:548–558.
8. **Davies, J., and A. Jimenez.** 1980. A new selective agent for eukaryotic cloning vectors. Am. J. Trop. Med. Hyg. (Suppl.)**29**:1089–1092.
9. **Fan, H., and I. Verma.** 1978. Size analysis and relationship of murine leukemia virus-specific mRNAs: evidence for transposition of sequences during synthesis and processing of subgenomic mRNA. J. Virol. **26**:468–478.
10. **Hentschel, C., J. Irminger, B. Bucher, and M. Birnstiel.** 1980. Sea urchin histone mRNA termini are located in gene regions downstream of putative regulatory sequences. Nature (London) **285**:147–151.
11. **Hwang, L.H., J. Park, and E. Gilboa.** 1984. Role of intron-contained sequences in formation of Moloney murine leukemia virus *env* mRNA. Mol. Cell. Biol. **4**:2289–2297.
12. **Laimins, L., G. Khoury, C. Gorman, B. Howard, and P. Gruss.** 1982. Host-specific activation of transcription by tandem repeats from simian virus 40 and Moloney murine sarcoma virus. Proc. Natl. Acad. Sci. U.S.A. **79**:6453–6457.
13. **Maniatis, T., P. Fritsch, and J. Sambrook.** 1982. Molecular cloning, laboratory manual. Cold Spring Harbor Laboratory, Cold Spring Harbor, N. Y.
14. **Mann, R., R. Mulligan, and D. Baltimore.** 1983. Construction of a retrovirus packaging mutant and its use to produce helper-free defective retrovirus. Cell **33**:153–159.
15. **Maxam, A., and W. Gilbert.** 1977. A new method for sequencing DNA. Proc. Natl. Acad. Sci. U.S.A. **74**:560–564.
16. **Mitra, S., M. Chow, J. Champoux, and D. Baltimore** 1982. Synthesis of murine leukemia virus strong stop DNA initiates at a unique site. J. Biol. Chem. **257**:5983–5986.
17. **Mount, S.** 1982. A catalogue of splice junction sequences. Nucleic Acids Res. **10**:459–472.
18. **Peters, G., F. Harada, J. Dahlberg, A. Panet, W. Haseltine, and D. Baltimore.** 1977. The low molecular weight RNAs of Moloney murine leukemia virus: identification of the primer for RNA-directed DNA synthesis. J. Virol. **21**:1031–1041.
19. **Pugatsch, T., and D. Stacey.** 1983. Identification of a sequence likely to be required for avian retroviral packaging. Virology **128**:505–511.
20. **Rautmann, G., H. Matthes, M. Gait, and R. Breathnach.** 1984. Synthetic donor and acceptor splice sites function in an RNA polymerase B (II) transcription unit. EMBO J. **3**:2021–2028.
21. **Rothenberg, E., D. Donoghue, and D. Baltimore.** 1978. Analysis of a 5′ leader sequence on murine leukemia virus 21S RNA: heteroduplex mapping with long reverse transciptase products. Cell **13**:435–451.
22. **Schwartzberg, P., J. Colicelli, and S. Goff.** 1983. Deletion mutants of Moloney murine leukemia virus which lack glycosylated *gag* protein are replication competent. J. Virol. **46**:538–546.
23. **Sharp, P.** 1981. Speculations on RNA splicing. Cell **23**:643–646.
24. **Shields, A., O. Witte, R. Rothenberg, and D. Baltimore.** 1978. High frequency of aberrant expression of Moloney murine leukemia virus in clonal infections. Cell **14**:601–609.
25. **Sorge, J., W. Ricci, and S. Hughes.** 1983. *cis*-Acting RNA packaging locus in the 115-nucleotide direct repeat of Rous sarcoma virus. J. Virol. **48**:667–675.
26. **Sorge, J., D. Wright, V. Erdman, and A. Cutting.** 1984. Amphotrophic retrovirus vector system for human cell gene transfer. Mol. Cell. Biol. **4**:1730–1737.
27. **Southern, P., and P. Berg.** 1982. Transformation of mammalian cells to antiobiotic resistance with a bacterial gene under control of the SV40 early region promoter. J. Mol. Appl. Genet. **1**:327–341.
28. **Treisman, R., S. Orkin, and T. Maniatis.** 1983. Specific transcription and RNA splicing defects in five cloned β-thalassemia genes. Nature (London) **302**:591–596.
29. **Varmus, H.** 1982. Form and function of retroviral proviruses. Science **216**:812–820.
30. **Watanabe, S., and H. Temin.** 1982. Encapsidation sequences for spleen necrosis virus, an avian retrovirus, are between the 5′ long terminal repeat and the start of the *gag* gene. Proc. Natl. Acad. Sci. U.S.A. **79**:5986-5990.
31. **Wieringa, B., E. Hofer, and C. Weissmann.** 1984. A minimal intron length but no specific internal sequence is required for splicing the large rabbit β-globin intron. Cell **37**:915–925.
32. **Wieringa, B., F. Meyer, J. Reiser, and C. Weissmann.** 1983. Unusual splice sites revealed by mutagenic inactivation of an authentic splice site of the rabbit β-globin gene. Nature (London) **301**:38–43.